DIABETIC RETINOPATHY CLASSIFICATION USING LENET-5 CLASSIFIER

[1*]Dr. C. Dhaya,
Professor, Department of Computer Science and Engineering, Adhiparasakthi Engineering College, Melmaruvathur, Tamil Nadu, India.

[2]Dr. B. Prakash,
Assistant Professor, Department of Computer Science and Engineering, SRM university, Kattankulathur, Tamil Nadu, India.
Corresponding Email ID: [1]dhaya@apec.edu.in*

Abstract

Generally diabetic retinopathy is a disorder that affects the retina of the eye and is caused by changes to the patient blood vessels. If diabetic retinopathy (DR) progresses to the macula and causes damage to it, diabetic macular edema may develop. Digital images of diseases must be manually examined by trained specialists for screening systems to be successful. Since screening is challenging and skilled personnel are in short supply, implementing efficient and effective treatment is considered costly. Automated systems solve such issues, but so far, their solutions have not been applicable to a wide variety of health conditions or real-world scenarios. In this paper, we use a LeNet classifier to classify the diabetic retinopathy from the input datasets. The model is designed in such a way that it achieves increased accuracy compared with conventional deep learning models.

Keywords: Diabetic retinopathy, LeNet-5, deep learning, classification
DOINumber:10.14704/nq.2022.20.8.NQ44927 **NeuroQuantology 2022; 20(8): 9071-9079**

1. Introduction

Blood glucose levels in diabetic patients are consistently higher than those in healthy individuals. Diabetics are more likely to experience complications with their eyes, (DR) is a retinal blood vessel disorder that mostly affects diabetics. Microaneurysms, hemorrhaging, and exudates are all signs of DR. Microaneurysms, seen on the retina as tiny red dots, are caused by irregularities at the artery edge. Damaged blood vessels create hemorrhages, which appear as dark red spots on the retina, while blocked arteries cause soft exudates, which appear as white lesions. Damage to one eyesight can be caused by either of these disorders. Waxy yellow patches on the retina are caused by hard exudates the body produces when there isn't enough blood in the arteries.

The two most frequent kinds of DR are proliferative DR (PDR) and non-proliferative DR (NPDR) [1]. The severity of NPDR, the most prevalent and introductory stage of DR, varies from person to person. When diabetic retinopathy progresses to the proliferative stage, aberrant new blood vessels form in the retina, a condition known as PDR. These new blood vessels develop abnormally, which increases the risk of them bursting and leaking fluid into the retina, which can cause permanent vision loss. DME is a form of DR that can occur during the spread of DR to the macula. DME causes a macula enlargement due to liquid buildup. The macula, located in the retina exact center, is the region of the eye responsible for sharp, central vision [2, 3]. The WHO predicts, percentage of people with DR will increase into 33% over the next few

years as the global prevalence of diabetes increases [4,5]. Increased vascular permeability is a hallmark of diabetic retinopathy, a complication that can develop from relatively benign abnormalities. As a result, new blood vessels may form, first on retina and then spreading to the vitreous gelsurface, causing a disorder called proliferative vitreoretinopathy (PDR). Unfortunately, DR is misdiagnosed as it progressed to a DME, at which point serious visual impairment has already occurred. This is a lengthy process that generally occurs after severe vision loss has occurred due to the disease.

The risk of blindness from diabetic retinopathy (DR) can be reduced by as much as 90 percent if the disease is detected and treated early[6]. Research has shown the importance of regular eye exams for diabetics, and laser photocoagulation has been proposed as a treatment option for patients with vision problems. Many real-world obstacles stand in the way of DR detection, however, including the need for human assessors, the sustainability of social and educational institutions, and the sustainability of financial organizations. Mild DR patients require any treatment, but they make sure their diabetes is managed. In order to catch DR early, it is crucial to monitor these indicators often.

Literature-based methods struggle to recognize and classify DR and DME when presented with extremes in lighting, color, size, and angle. They also have trouble generalizing their limited experience to novel contexts. The first stages of DR are characterized by extremely minute lesions that are not readily detectable by the currently available diagnostic tools. In this work, we used Custom LeNet-5 to investigate the threat of DR and DME, successfully overcoming the challenges faced by previous attempts. LeNet-5 network was selected to aid in the computation of deep features learned from fundus samples. High-magnification retinal imaging provides a window into the eye interior, making it possible to spot irregularities related to DR and DME.In this paper, we use a LeNet classifier to classify the diabetic retinopathy from the input datasets.

2. Related works

There have been a number of machine learning methods developed for the detection of DR in retinal images. The placement and naming of DR lesions was proposed by Imani et al. [7]. The first step is to apply an Otsu thresholding technique to the input image in order to separate the green channel and remove any noise or other unwanted features. In the next stage, features are extracted from the images using morphological component analysis (MCA) to be used in the training of a support-vector machine (SVM) classifier. However, the method may not be applicable to post-processed samples despite its superior performance compared to the difficult database.

Seoud et al. [8] demonstrated that using the idea of dynamic form features can lead to an automatic classification of DR lesions. (DSF). An octagonal matching filter is used to extract the characteristics, and a ring-shaped filter of varying scales is also employed. An RF classifier is used to perform the separation. Even when input samples vary in terms of illumination and resolution, the approach described is able to detect lesions with outstanding precision. The method has one major drawback, however: it can only spot red lesions.

In [9], we use a hand-coded model that combines a Gaussian data description (GDD) with wavelet transform to produce key points that can be used to differentiate between different stages of DME. The connection between the primary elements was identified using this technique.

Using fundus images as their major source of data, Zou et al. [10] developed a technique for diagnosing DME. Using the input sample characteristics and geographic information, a support vector machine (SVM) is combined with Bayesian probability theory to help zero in on the DME. The method described is useful for processing images with DME, although there is potential for improvement in terms of performance.

Using a Gaussian filter bank and a differential Gaussian filter bank, Marin et al. [11] devised a technique for finding DMEs. In order to classify each of the possible DME locations, a local regression classifier is used. The method described is effective for DR screening, however it has room for improvement.

Li et al. [12] reported fresh fundus samples using the DDR dataset, which was used by five different deep learning (DL) based categorization and segmentation frameworks. The DDR dataset included these samples for analysis. In terms of DME classification and segmentation, DL-based algorithms excel. However, these methods need further work to be effective for smaller lesions.

Perdomo et al. [13] published a novel approach to DR screening that makes use of a two-stage CNN architecture. By first extracting deep characteristics from the input sample using an eight-layer CNN framework, the AlexNet architecture is trained to distinguish between images with and without DME. This instructs the system to recognize the difference between photos with and without DME.

With the DL method, Gargeya et al. [14] were able to create a fully automated framework for DR recognition. For the purpose of automating DR detection, Abramoff et al. [15] created a DL approach. According to the authors, the procedure outperformed more conventional, hand-coded methods.

Tan et al. [16] developed a CNN architecture for identifying and classifying exudates, hemorrhages, and microaneurysms. Although a lot of theoretical work has been published for DR screening, it is still important to look at how well these techniques work in practice. The current methods for identifying DR and DME might stand to be improved upon.

3. Proposed Method

The study can be broadly categorized in two ways. Our process begins with dataset preparation, then continues with an upgrade to the LENET-5 network, formerly used to categorize diseases of the eye. Producing annotations for disease photographs to emphasize the precise location of concern is the first step before training LeNet-5 over the annotated data.

For this purpose, we trained a proprietary LeNet-5 network on top of a DenseNet-100 base. To function properly, the Custom LeNet-5 framework DenseNet-100 features extractor requires a preview of the input image as well as the location and size of the affected region

.

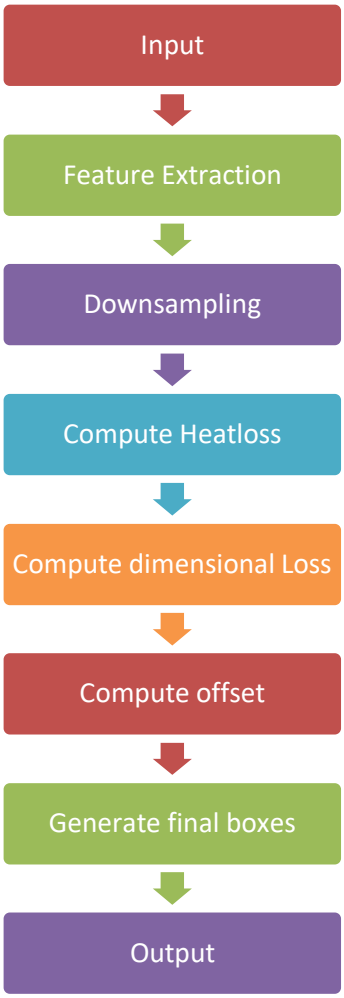

Figure 1: Proposed LeNet Model

The system architecture that the proposed process will use is shown in Figure 1. Two of the first parameters for DenseNet-100 are the input sample and the bounding box (bbox). The Bbox job is to find the ROI inside the CNN data points. Once locations are identified, the Custom LeNet-5 is then trained to assign classes to those locations. Finally, estimates of the precision of each unit have been provided. All of these estimations are based on metrics currently employed in computer vision.

Annotations

In order to have a productive training session, it is crucial to pinpoint the precise location of the damaged region using the input retinal samples. Use a microscope for this purpose. The illustrative annotations for this procedure were developed using the program LabelImg. An XML file is created and used to store the generated annotations. This file contains (I) the category associated with affected location, and (ii) box values that can be used to sketch a box around the detected area. Following the initial step of creating an XML file, the next step is to convert the file into a training record file for use in the model education.

LeNet-5

Figure 2 shows that there are a total of seven tiers in the LeNet-5 architecture. There is one fully connected layer (F6), three convolutional layers (C1, C3, and C5), two pooling layers (S2 and S4), an output layer, and a third pooling layer.

Initially, the LeNet-5 architecture took advantage of a 32321-pixel image for handwritten number recognition. 6 filters, each of size five and stride one, were used in the convolution. In the end, feature map with these specs: 28x28x6. The dimensions were

consequently lowered to a more manageable 14 x 14 x 6 inches. In addition, a convolutional layer was utilized that included with stride filters. The 120 feature maps that go into C5 convolutional layer are quite impressive.

Its dimensions are as follows, and it contains 120 neurons coupled to the 400 nodes in the layer below it (5x5x16). This F6 layer consists of eighty-four individual units. C5, the fifth convolutional layer, is fully connected and has 120 units. For each of the 84 categories, the output layer employs Euclidean Radial Basis Function (RBF) units.

$$y_i = \sum_j \left(x_j - w_{ij} \right)^2$$

where

W_{ij}refers toi^{th} parameter vector,

$y_i$refers toi^{th} RBF unit, and

$x_j$is the value of the j^{th} input vector unit.

LeNet is easier to implement, works well with parallel hardware, and efficiently completes tasks of moderate size for image recognition.It had a 92-99% success rate while taking images despite challenging backgrounds, different sizes, poor lighting, and incorrect orientation. LeNet diagnostic accuracy for olive rapid decline syndrome has improved dramatically with the latest update, reaching an astounding 99%. Images of wilted cucumber leaves are processed using a network with the same architecture as LENET-5.

It takes less time to train the LeNet model and less storage space after it finished, but the model is not good. When the RELU activation function is used, the gradient decreases.

Properly dividing eye diseases into their many subtypes necessitates the rapid and precise calculation of crucial points. Despite this, there are many obstacles that might make constructing a discriminative set of feature vectors a lengthy and difficult process. Over-fitting occurs when models employ a large number of key-point vectors. However, if only a few landmarks are used, the method risks failing to pick up on important object behaviors, such as alterations in texture and color, that render unhealthy regions indistinguishable from healthy ones.

In order to reach a conclusion, you can compare the computed peaks to the heatmaps for each class individually. Only the top 100 responses were chosen, but only if their value was more than or equal to the values of their 8 linked neighbors. So, we can suppose that the *N* centers of Category *C* that have been discovered are being displayed in *Q*, as indicated by Equation (2).

$$Q = \left\{ \left(x_j, y_j \right) \right\}_{j=1}^{N}$$

where (x_j,y_j) is an integer pair representing the coordinates of each detected hotspot. Our method uses Equation (3) to build the final bounding box by factoring in the values of all the keypoints ($O_{x,y}$). To what extent can we trust this identification is accurate is something we can now measure.

$$\begin{pmatrix} x_j + \partial x_j - \frac{w_j}{2}, y_j + \partial y_j - \frac{h_j}{2}, \\ x_j + \partial x_j + \frac{w_j}{2}, y_j + \partial y_j + \frac{h_j}{2} \end{pmatrix}$$

where

$(\partial x_j,\partial y_j)$- offset estimate from $O_{x,y}$ and

(w_j,w_j) - prediction size from $d_{x,y}$. The bounding box is calculated from the predicted features, eliminating the need for non-maxima suppression.

Batch Gradient Descent (BGD) Optimization

To adjust the parameter *x*, this method uses the entire training dataset as a search space, as shown in Equation (4). Gradient calculations for training datasets with millions or billions of samples are time-consuming. It might also be challenging to feed all of the samples into a model simultaneously due to the limited memory available in computers.

Because of these limitations, the batch gradient descent approach is not recommended for updating the parameters of a deep learning model. These values are related to the current iteration1 to *n*.

$$x_{k+1}=x_k-t_k\Delta f(x_k)^{(1:n)}$$

4. Results and Discussions

An AI system can function independently as a fully automated system, or it can assist in a more traditional semi-automated setup. It is crucial for determining when a DL algorithm starts producing useful results. The sensitivity and specificity of the system must be taken into account while setting the operational threshold of the fully automated system. Achieving high sensitivity requires careful attention to specificity so that unnecessary hospital visits are not triggered. The consequences may be terrible if specificity is severely degraded. For countries with established DR screening systems using manual graders, the assistive semi-automated approach may be an appropriate alternative strategy because it may help to reduce the requirement for human labour. This is due to the fact that the model can aid in doing less work for humans.

To allow the human graders to undertake a secondary grading on the images that have been found to be referable, the DL algorithm can be tuned to have a high sensitivity threshold. This will allow us to eliminate the usual, non-referable retinal images. This combined strategy has the potential to lessen the need for human intervention during manual grading while still achieving high levels of sensitivity and specificity.

Dataset

The Kaggle EyePACS dataset contains over 80,000 fundus images from the EyePACS platform. The diabetic retinopathy classification community relies heavily on this dataset, as it is the gold standard in terms of size and accessibility. Structured from numerous high-resolution fundus images of the retina, both eyes. These images were captured with various imaging modalities and equipment at primary care clinics in California and elsewhere. The blurring, artifacts, exposure, and focusing issues in the data and the ground truth labels are all deliberate attempts to more closely mimic real-world scenarios. An expert used the ICDRDSS scale to assign ratings to the images.

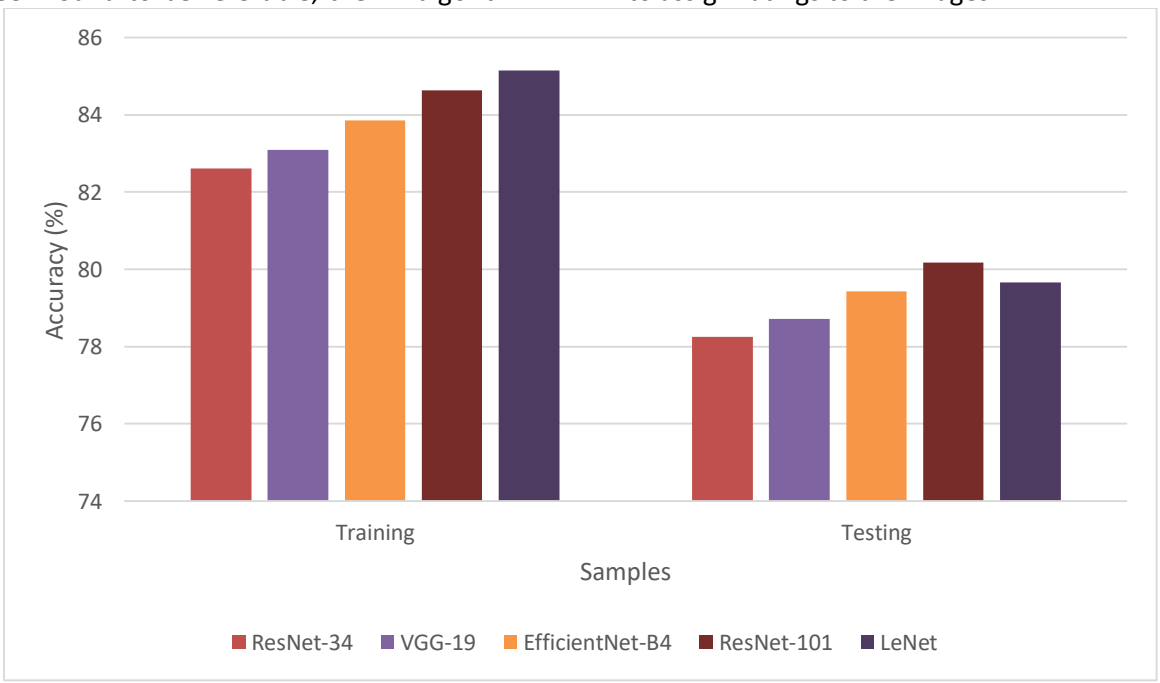

Figure 2: Accuracy

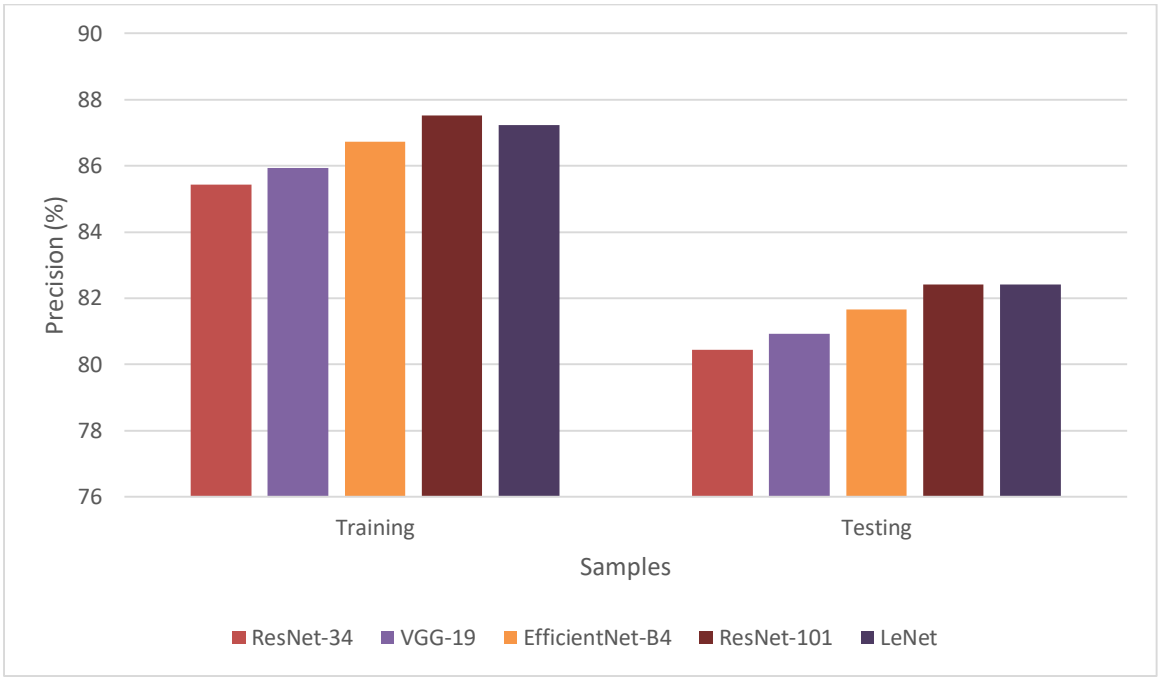

Figure 3: Precision

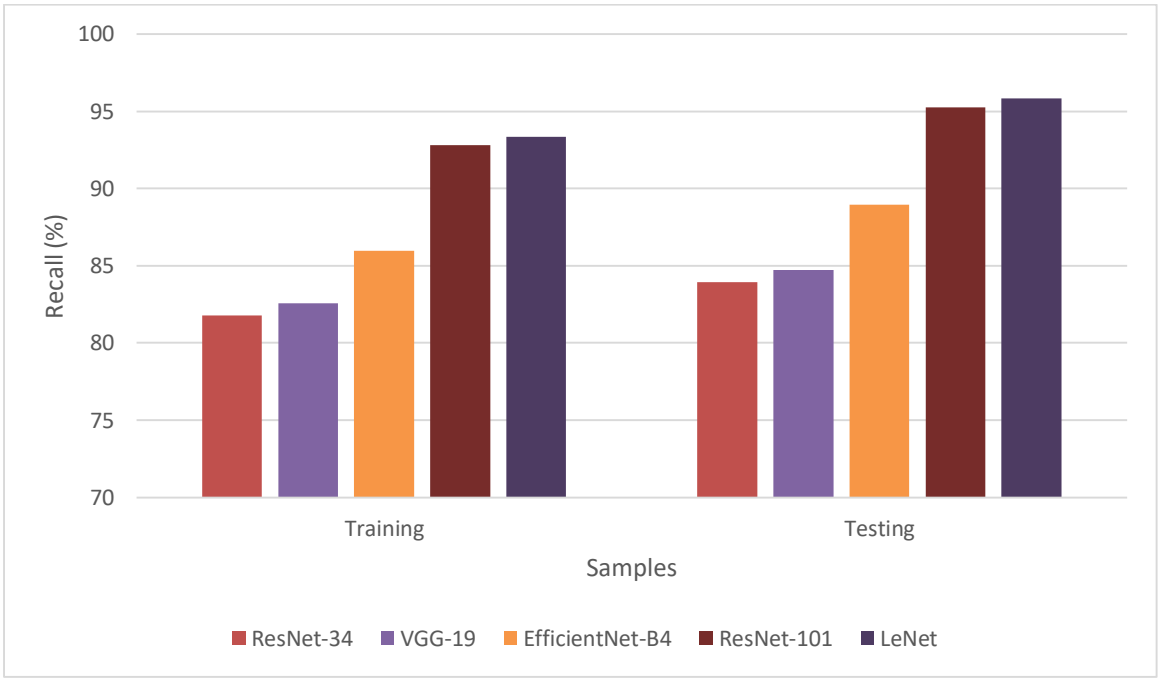

Figure 4: Recall

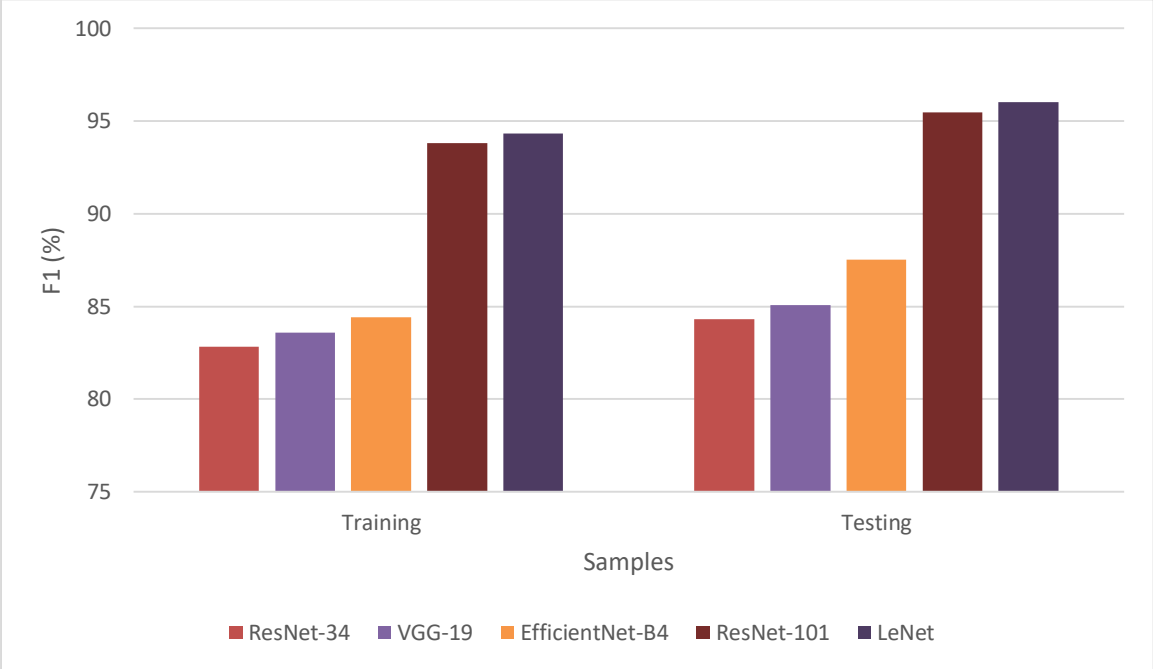

Figure 5: F-Measure

The DL models are analysed on the reliability of medical diagnoses were reviewed by our group. Each of these analyses verified the deep learning method effectiveness by testing it with new data or on a previously existing patient population. An overwhelming majority of patients (90%) chose an automated deep learning model to human grading, as found by a study that evaluated both diagnostic accuracy and patient happiness.

The relevant features are used by the trained model to tell the normal and DR classes apart in the test data. In addition, the test set predicted labels were compared to the gold-standard labels, and the classifier accuracy, sensitivity, and specificity were calculated.

5. Conclusions

Our proposed methodology outperforms state-of-the-art approaches, as evidenced by both qualitative and quantitative results, thanks to LeNet-5 higher localization capacity, which can swiftly recognize tiny lesions with training data. One of the main advantages of the method we have developed is that it can accurately identify and categorize illness lesions. The ability of our method to accurately extract essential characteristics from images with low brightness and a lot of noise sets it apart from existing state-of-the-art DR and DME classification systems. As a result, our approach has the potential to be employed for the automatic detection and characterization of DR and DME lesions.

References

[1] Sri, K. S., Priya, G. K., Kumar, B. P., Sravya, S. D., & Priya, M. B. (2022, April). Diabetic Retinopathy Classification using Deep Learning Technique. In *2022 6th International Conference on Trends in Electronics and Informatics (ICOEI)* (pp. 1492-1496). IEEE.

[2] Sri, K. S., Priya, G. K., Kumar, B. P., Sravya, S. D., & Priya, M. B. (2022, April). Diabetic Retinopathy Classification using Deep Learning Technique. In *2022 6th International Conference on Trends in Electronics and Informatics (ICOEI)* (pp. 1492-1496). IEEE.

[3] Mathews, M. R., & Anzar, S. M. (2021). A comprehensive review on automated systems for severity grading of diabetic retinopathy and macular edema. *International Journal of Imaging Systems and Technology*, *31*(4), 2093-2122.

[4] Shanthini, A., Manogaran, G., & Vadivu, G. (2023). Deep Convolutional Neural Network Architecture. In *Deep*

Convolutional Neural Network for The Prognosis of Diabetic Retinopathy (pp. 37-45). Springer, Singapore.

[5] Al-Smadi, M., Hammad, M., Baker, Q. B., & Sa'ad, A. (2021). A transfer learning with deep neural network approach for diabetic retinopathy classification. *International Journal of Electrical and Computer Engineering*, *11*(4), 3492.

[6] Kumar, M. S., Anu, V. M., & Shiva, M. (2022). *Retinal Image Processing Using Neural Networks with Deep Learning* (No. 7580). EasyChair.

[7] Imani, E., Pourreza, H. R., & Banaee, T. (2015). Fully automated diabetic retinopathy screening using morphological component analysis. *Computerized medical imaging and graphics*, *43*, 78-88.

[8] Seoud, L., Hurtut, T., Chelbi, J., Cheriet, F., & Langlois, J. P. (2015). Red lesion detection using dynamic shape features for diabetic retinopathy screening. *IEEE transactions on medical imaging*, *35*(4), 1116-1126.

[9] Baby, C. G., & Chandy, D. A. (2013, February). Content-based retinal image retrieval using dual-tree complex wavelet transform. In *2013 International Conference on Signal Processing, Image Processing & Pattern Recognition* (pp. 195-199). IEEE.

[10] Zou, X., Zhao, X., Yang, Y., & Li, N. (2016). Learning-based visual saliency model for detecting diabetic macular edema in retinal image. *Computational intelligence and neuroscience*, *2016*.

[11] Marín, D., Gegundez-Arias, M. E., Ponte, B., Alvarez, F., Garrido, J., Ortega, C., ... & Bravo, J. M. (2018). An exudate detection method for diagnosis risk of diabetic macular edema in retinal images using feature-based and supervised classification. *Medical & biological engineering & computing*, *56*(8), 1379-1390.

[12] Poplin, R., Varadarajan, A. V., Blumer, K., Liu, Y., McConnell, M. V., Corrado, G. S., ... & Webster, D. R. (2018). Prediction of cardiovascular risk factors from retinal fundus photographs via deep learning. *Nature Biomedical Engineering*, *2*(3), 158-164.

[13] Perdomo, O., Otalora, S., Rodríguez, F., Arevalo, J., & González, F. A. (2016, October). A novel machine learning model based on exudate localization to detect diabetic macular edema. In *Ophthalmic Medical Image Analysis International Workshop* (Vol. 3, No. 2016). University of Iowa.

[14] Gargeya, R., & Leng, T. (2017). Automated identification of diabetic retinopathy using deep learning. *Ophthalmology*, *124*(7), 962-969.

[15] Abràmoff, M. D., Lou, Y., Erginay, A., Clarida, W., Amelon, R., Folk, J. C., & Niemeijer, M. (2016). Improved automated detection of diabetic retinopathy on a publicly available dataset through integration of deep learning. *Investigative ophthalmology & visual science*, *57*(13), 5200-5206.

[16] Tan, J. H., Fujita, H., Sivaprasad, S., Bhandary, S. V., Rao, A. K., Chua, K. C., & Acharya, U. R. (2017). Automated segmentation of exudates, haemorrhages, microaneurysms using single convolutional neural network. *Information sciences*, *420*, 66-76.

*e*ISSN1303-5150